

DOI: 10.1002/adem.((please add manuscript number))

Impact of surface treatment and morphology of diamond thin films on neuron adhesion

By *Barbora Jakubcová, Jana Turňová, Ondřej Řehounek, Jiří Polák, Andrea Mineva, Andrew Taylor, Pavel Hubík, Václav Petrák and Vladimíra Petráková**

*Vladimíra Petráková Corresponding-Author, Barbora Jakubcová, Jana Turňová, Ondřej Řehounek, Jiří Polák, Andrea Mineva, Václav Petrák
Faculty of Biomedical Engineering, Czech Technical University in Prague, nam. Sitna 3105, 272 01, Kladno, Czech Republic*

E-mail: vladimira.petrakova@fbmi.cvut.cz

*Andrew Taylor, Pavel Hubík
Institute of Physics, Czech Academy of Sciences, Na Slovance 2, 182 21, Prague, Czech Republic*

Acknowledgments: This work was supported by the Czech Science Foundation Grant No. – 17-15319S and by CTU grant No. SGS16/191/OHK4/2T/17.

Abstract: The ability to form an efficient interface between material and neural cells is a crucial aspect of the construction of neuroelectrodes. Diamond offers material characteristics that could, by a large extent, improve the performance of neuroelectrodes. The greatest advantage of diamond is a large variety of material and surface properties such as electrical conductivity, surface morphology, and surface chemistry. Such a variety of material characteristics can lead to various cellular responses. Here we compare survival, adhesion, and neurite formation of primary neurons on diamond thin films of various morphology and on their treatment with several types of polymers commonly used to enhance cell adhesion. We found that the variation of surface roughness of nanocrystalline diamond film does not have a major influence on the neuron survival or adhesion. The adhesion of neurons can be influenced by the selected type of polymer coating. High molecular weight of polyethylenimine resulted in lower viability, adhesion and neurite formation. The addition of laminin to treated films did not lead to significant improvements in neuron adhesion and neurite development. Our findings emphasize the importance of the correct

polymer treatment over morphological properties of diamond thin films as a material for forming interfaces with primary neurons.

1. Introduction

The successful construction of neuroelectrodes is mainly given by the ability to create an efficient interface between the electrode material and neural cells or tissues. Recently, diamond became an attractive material of choice for construction of neuroelectrodes^{1,2} and neurointerfaces³⁻⁷ and their applications as retinal prosthesis^{8,9}. The material characteristics of diamond combines several aspects that could improve the performance of neuroelectrodes. These characteristics are mechanical and chemical stability, which lead to longer durability in harsh biological environments and to higher biocompatibility^{10,11}, tunable conductivity enabled by chemical vapour deposition (CVD) synthesis, the doping level¹²⁻¹⁴, and variable surface morphology given by various grain size. The use of nanopatterning or lithography that could promote the cell adhesion to the surface or direct the cell growth¹⁵⁻¹⁸.

Diamond thin films have been considered for biomedical and clinical applications since the 1990s when great progress in the CVD technology and understanding of the growth process of diamond^{19,20} enabled coating of a large variety of materials used in medicine^{21,22}. The applications focused mostly on dental and orthopedic implants or stent implants with the goal to increase mechanical resistance and biocompatibility²³⁻²⁵. Despite the large effort, only a very limited number of diamond-coated clinical products are yet on the market. Compared to coatings of dental or orthopedic implants, construction of efficient and competitive neuroelectrode is much more complex and challenging. Even though many scientific groups are working on this task, the concept of a diamond as a neuroelectrode is still new and some of the fundamental questions remain open. As an example, only recently (and after more than 10 years after first articles

appeared on this topic) it was rationally explained why primary neuron cultures fail to grow on the bare diamond surface²⁶. Optimisation of neural adhesion to the electrode surface is of major importance for assessment of neural cells and tissues in vitro, such as microelectrodearrays (MEAs). In such case, neurons are cultured directly on the MEAs material without the presence of other cells that secrete and express extracellular matrices and cell adhesion molecules that result in enhanced cell adhesion to the material.

Nanocrystalline diamond can significantly improve performance of MEAs. Performance of all-diamond electrodes was successfully evaluated recently^{27,28}. Nanocrystalline diamond (NCD), when doped by boron (BDD), exhibit exceptional electrochemical properties. Conductive BDD has the largest potential window (> 3 V), low background current, exceptional mechanical and chemical stability, durability, and tunable surface chemistry. The sensitivity and performance of BDD electrode can be further enhanced by nanostructuring^{29,30}. Moreover, diamond could serve as a platform for dual-mode electrode, combining detection of chemical and electrical activity.

The greatest advantage of diamond is a large variety of material and surface properties such as electrical conductivity, surface chemistry, and surface morphology that allows to boost material properties to optimize electrode performance for desired application in combination with extreme chemical resistance and durability. The diversity in material properties can play a role in the cellular response. There were many studies on evaluating the influence of various parameters of diamond films on neuron interfacing, recently summarized in⁷. The studies focused on the effect of surface termination (hydrogen vs oxygen termination³¹), level of doping³², and surface morphology^{1,33}. It is difficult to make general conclusions about the influence of one aspect or the other, as in some cases the results contradict each other. The necessity of adhesion promoting polymer coating was a subject of wide discussion with often conflicting results. It is, for example,

still not clear to what extent the adhesion and development of neurons is influenced by the properties of the diamond film itself or by the use of surface treatment with adhesion promoting polymers. Here we address this problem. We compare development of primary neural cells on diamond thin films of various morphology and of various chemical treatment using several types of polymers commonly used to enhance adhesion.

2. Materials and Methods

2.1. NCD preparation

Nanocrystalline diamond (NCD) layers were grown on glass substrates using a microwave plasma enhanced chemical vapour deposition system with linear antenna delivery (MW-LA-PECVD) that allows large area diamond growth and preparation of multiple samples per deposition³⁴. Prior to growth of NCD layers, glass substrates were seeded with a detonation diamond nanoparticles solution (NanoAmando®, NanoCarbon Research Institute Ltd) using spin coating method, as described in detail elsewhere³⁴. Deposition conditions are reported in **Table 1**. The addition of nitrogen into the gas chemistry is known to increase re-nucleation during the growth process³⁵, leading to the growth of so called ultra nanocrystalline diamond layers, which possess lower crystal size and differs in the surface morphology. In addition boron doped nanocrystalline diamond layers on silicon and glass substrates were produced in an ASTeX 5010 (Seki Technotron, Japan) microwave plasma enhanced chemical vapour deposition (MW PE CVD) reactor¹⁴, see Table 1. for growth conditions.

Table 1. Growth conditions of nanocrystalline diamonds (with RMS = 13.6 nm (NCD1), nanocrystalline diamond with RMS = 16.1 nm (NCD2) and nanocrystalline diamond with RMS = 31.9 nm (NCD3). In one deposition, more than ten samples were prepared. For neuron growth, triplicates of nanocrystalline diamond samples were used.

	ND1	ND2	ND3
Microwave power (kW)	3	3	1.25

CH4 (%)	4.7	5	1
H2 (%)	87.6	92	99
CO2 (%)	2.9	3	0
N2 (%)	4.7	0	0
B/C (ppm)	0	0	4000
Process pressure (mbar)	0.3	0.3	51
Deposition time (h)	8	8	2
Deposition rate (nm / h)	62	44	200

2.2. Gold films preparation

Gold films were deposited on glass substrates from Au pellets (5N purity, Kurt J. Lesker) in Edwards AUTO 500 multipurpose vacuum system by means of electron-beam evaporation. Prior to evaporation the substrates were cleaned by isopropyl alcohol for 5 min and washed with distilled water, boiled in deionized water (Milli-Q) for 5 min and dried). Immediately before loading into the vacuum system, the substrates were blown using pure dry nitrogen. For improvement of adhesion, 10 nm Ti films were evaporated first to serve as an interlayer between glass and gold. Subsequently, without breaking vacuum, 100 nm Au films were deposited. Both evaporation steps were performed in clean (no hydrocarbon lubricant present) vacuum of $(1-3) \times 10^{-6}$ Pa.

2.3. Sample treatment and polymer coating

All diamond samples were oxidized using oxygen plasma immediately after growth to ensure oxygen termination that leads to high hydrophilicity that improves the homogeneity of further polymer coatings. If not stated otherwise, all samples were cleaned as described above. The samples were sterilized with dry-heat oven (160 °C, 120 min).

Polymer coating was carried out using polyethylenimine (PEI) with molecular weights of 800, 2000, 750000 g mol⁻¹ (Sigma Aldrich) and poly-D-lysine (PDL, Sigma Aldrich)

with/without Laminin (Sigma Aldrich). All the PEI solutions were diluted with borate buffer (pH 8.4) to a concentration of 0.05 to 0.1 wt. %. The borate buffer was prepared from boric acid (3.10 g) and borax (4.75 g) dissolved in distilled water (80 °C, 1 l). PDL was diluted with distilled water to a concentration of 0.1% work solution. Samples were incubated with polymer solution for 1 hour at room temperature. Then samples were rinsed 10× with sterilized distilled water. Stock laminin solution (Sigma Aldrich, final concentration of 20 $\mu\text{g ml}^{-1}$ in plating medium) was added on samples with PDL and PEI 2000 and was incubated for 30 min at 36 °C prior to cells seeding, then aspirated and cells were plated directly. For all samples, we used the same procedure of chemical treatment (PEI/PDL coating for 1 h). The homogeneity of coatings was verified by single molecule fluorescence microscopy by measurement of polymer autofluorescence on treated substrates. The polymer coating affected the roughness of studied diamond thin films by less than 2nm for PEI2000 coatings (Supporting Information Figure S7).

2.4. Surface analysis

Surface morphology was measured by a field emission scanning electron microscope (SEM) FEI Quanta 3D FEG. Raman spectroscopy was carried out at room temperature using a Renishaw InVia Raman Microscope at a wavelength of 488 nm and a laser power of 6 mW at the sample. Surface roughness was examined also by atomic force microscopy (AFM) - JPK Instruments model NanoWizard® 3 NanoScience AFM, using the semi contact mode operated at room temperature and a scan area of 5x5 μm . The surface root-mean-square (RMS) roughness was calculated as:

$$RMS = \sqrt{\frac{y_1^2 + y_2^2 + \dots + y_n^2}{n}} = \sqrt{\frac{1}{n} \cdot \sum_{i=1}^n y_i^2} = \sqrt{\overline{y^2}}, \quad (1)$$

where y_i^2 are pixel values from the AFM, More precisely, it is the height of each pixel, $\overline{y^2}$ denotes the mean of the values y_i^2 .

Measured data were processed in the program JPK Data Processing version spm-5.0.78 (JPK Instruments). The data presented in this paper show the image surface (measured profile height), profile graph of the measured deflection offset each for a section taken horizontally in the middle of the image and RMS value.

2.5. Cell culture

Rat embryonic (day 18) cortex neurons were isolated and cultivated as previously described³⁶. Time-pregnant (day 18) female outbred albino Wistar rat (*Rattus norvegicus*) was euthanized according to the law no. 246/1992 of the Czech Republic. The embryonic cortex was removed. Neurons were isolated by dissociation with isolation kit Neuron Isolation Enzyme with papain (Thermo Scientific) and mechanical trituration in Hank's buffered saline solution (HBSS, Gibco). Cortical cells were gently resuspended in serum-free Neurobasal medium (Neurobasal Medium, Life Technologies) supplemented with 0.25 % GlutaMax (Gibco), 2 % B27 (Gibco) and 0.2 % gentamicin (Sandoz). The B27-supplement suppresses the glial cells growth to achieve < 0.5% of the glial cells in the culture³⁷. After separation and cleaning steps the cells were centrifuged (5 min, 1000 rpm), counted and plated onto samples coated with PEI, PEI+laminin or PDL, PLD+laminin at a density from 0.5×10^6 to 1×10^6 cells per 1 ml in a volume 100 μ l (glass) and 50 μ l (nanocrystalline diamond). The medium was replaced 24 h after culturing day in vitro (DIV1) with fresh Neurobasal medium, and then half of the maintenance medium was replaced every 3-4

days. Cortex neurons were kept at 36 °C in humidified atmosphere of 5% CO₂. Cultures were kept until DIV12 to DIV19 day.

2.6. Fluorescent staining

LIVE/DEAD® Viability/Cytotoxicity Kit for mammalian cells (ThermoFisher Scientific Inc.) was used for evaluation and verification of cells viability. Cells were rinsed twice with Dulbecco's phosphate-buffered saline (Sigma Aldrich). Subsequently 100-150 µl LIVE/DEAD® reagents prepared according the manufacturer's instructions was added and cells was incubated for 15 min at room temperature. Finally, the reagents were removed, cells were rinsed once with phosphate-buffered saline and cells were analysed. The kit includes two fluorescent dyes: calcein AM with $\lambda_{em} = 515$ nm (it stains live cells) and ethidium homodimer $\lambda_{em} = 617$ nm (it stains dead cells).

2.7. Imaging

Microscopic analysis of cells was performed using an optical microscope Optika XDS-1R with a digital camera Optikam B3. Microscope was equipped with a phase contrast objectives 40x/0.65, 25x/0.40 and 10x/0.25. Inverted microscope (Olympus IX73) equipped with X-cite® 120Q excitation light source was used for fluorescence imaging.

For each sample triplicate, number of photos were made (>10) on random locations to analyze over 100 cells for each parameter. The overall statistics was performed from at least eight independent measurements. Statistical analysis was performed using one-way analysis of variance (ANOVA) on data for the last day of cultivation to determine whether there are any statistically significant differences between the means of studied parameters.

2.8 Evaluation of neuron adhesion

From captured images (example on **Figure S1a**), we extracted four parameters: viability, cell area, neurite number per cell, neurite length per cell in photo. The viability represents the percentage of live cells over the sum of the cells. The cell area represents the area of live cells normalized to the number of live cells in image. These two parameters represent the survival of cells on the surface and their adhesion to the surface. Number of neurite and the length of neurite was normalized to the number of cells in the picture. This parameter represents the ability of neurons to develop neural connections and networks. The viability and the cell area was calculated using the script written for MATLAB (MathWorks) using Image Processing Toolbox. Length and number of neurites was examined using ImageJ (MacBiophotonics) with the NeuronJ plugin.

The disadvantage of this method is a considerably low contrast of the cells in images compared to the background and, in our case, also disturbing optical artefacts related to the limitations of the equipment. To verify the accuracy of such analysis, some of the samples were stained with LIVE/DEAD® Viability/Cytotoxicity Kit for mammalian cells and observed in the fluorescence microscope (Figure S1b). This kit provides information about the functional status of the cell by detecting cytoplasmic esterase activity³⁸.

3. Results and discussion

In this paper, we show how the surface roughness of nanocrystalline diamond (NCD) films and the selection of a polymer used for the treatment of NCD films affects the viability of cortex neurons, formation of neurites and their adhesion to the surface. We compare three different types of material commonly used for neural cell culturing; glass, gold and NCD. We further focus on the optimization of the surface treatment and evaluate the impact of the selection of the

polymer on the viability and adhesion of neurons on NCD films. In the last section, we compare cortex neurons cultured on NCD films with various surface roughnesses.

To observe the trend of the cell adhesion and development during the first 12 days, we chose the minimal invasive method to analyze cells and used phase-contrast transmission optical microscopy. This approach allowed us to monitor the dynamics of studied characteristics and quantitatively compare the influence of material characteristics (surface roughness) and surface treatment on neuron characteristics. In the following sections, we present parameters named above, which describe the cellular response. Each experiment focused on comparison of one aspect of material/surface characteristic and was performed on the same neuron culture. Due to the variation of the neuron cultures it is not possible to directly compare absolute values between sets of experiments (for example results in the section 3.1 with results in section 3.2). Neurons were cultured under such conditions that suppressed the growth of glia cells (see Material and Methods section 2. 5 for details).

3.1 Initial comparison of glass, gold and diamond surface

As an initial experiment, we cultured neurons on three different types of material: glass, gold and NCD film. Glass was used as a control for all experiments. Gold was selected as a material that is commonly used to construct neuroelectrodes^{38, 39}. The goal was to verify that NCD is in general suitable for neuron culturing. Selected materials differ in surface roughness and conductivity. All substrates were treated by polyethylenimine ($M_w = 2000 \text{ g mol}^{-1}$)

Figure 1. shows surface morphology of samples and variations in surface roughness. Measurements was performed by AFM and calculated values of surface roughness are presented in **Table 2.**

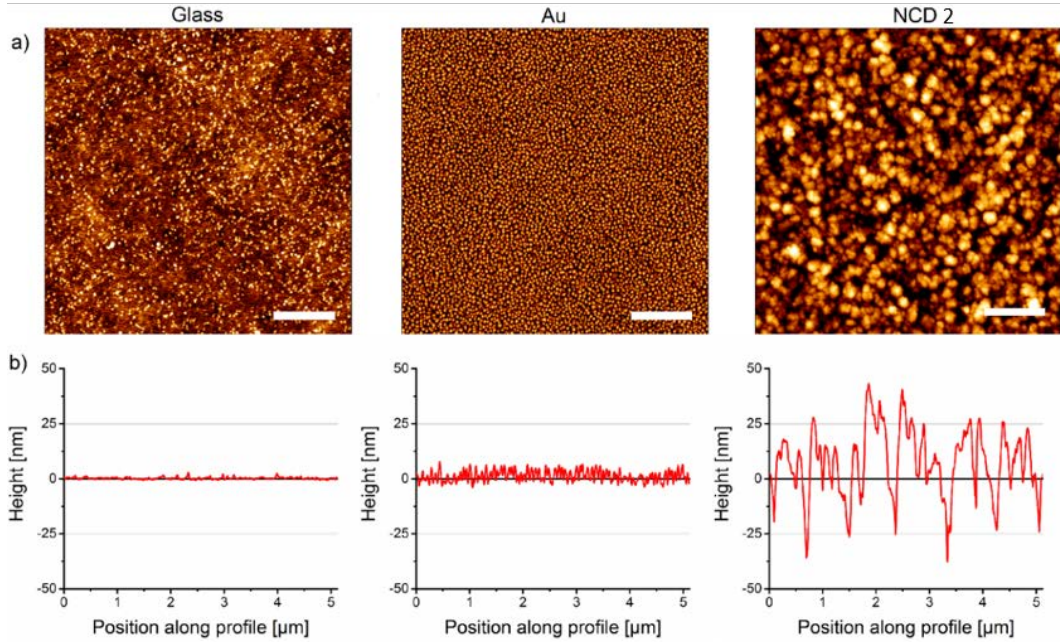


Figure 1. Materials differ in surface morphology and roughness. (a) AFM images of average roughness measured on glass, gold (Au) and nanocrystalline diamond (NCD2). Scale bar = 1 μm, (b) AFM profiles of the glass, Au and ND respectively (5 μm section taken horizontally across the middle of image).

Table 2. Measured RMS values of different substrates used for neurons culturing. Standard deviance of three independent measurements is given.

Material	RMS (nm)
Glass	0.5 ± 0.2
Gold	2.4 ± 0.3
NCD2	16.1 ± 1.1

The trend of the cell culture is shown on **Figure 2**. Data showed that neurons were able to adhere and develop on all samples. We observed high viability of cultured neurons, increase in the cell area and neurite formation over 20 days of cultivation. This indicates a low rate of cell death and adhesion of neurons on all materials.

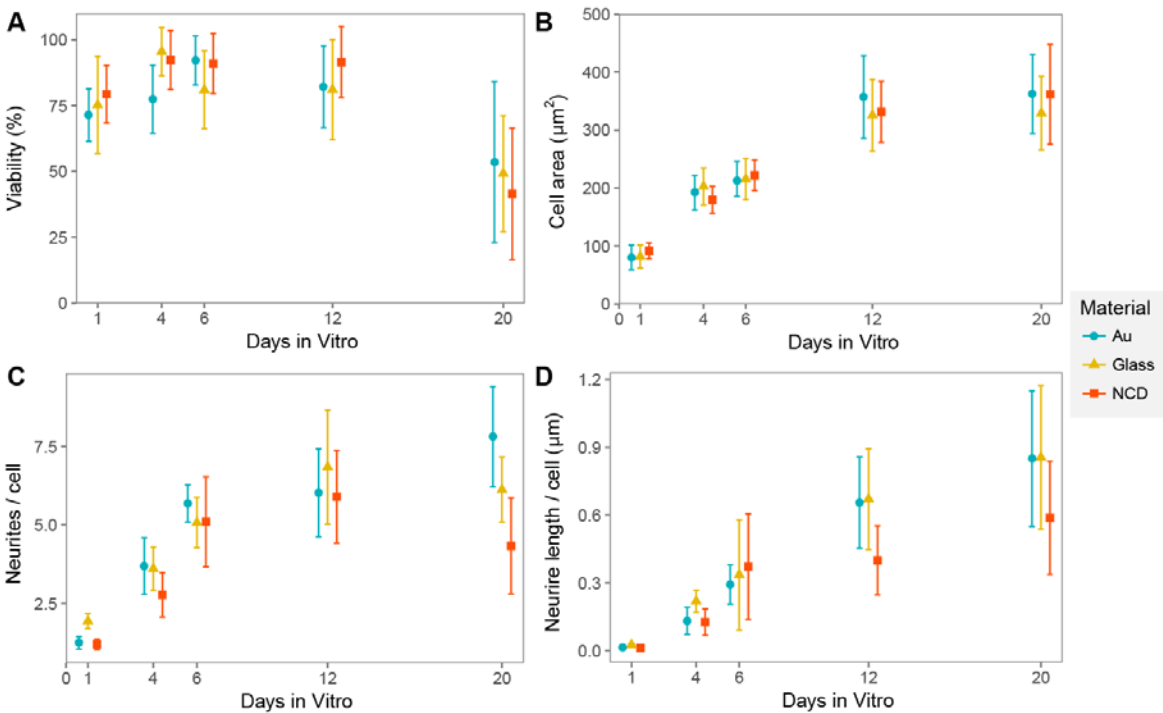


Figure 2. Characteristics of neurons on diamond thin films is comparable to gold and glass. Graphs show the results from neuron culturing on glass, gold and nanocrystalline diamond (NCD2) in following parameters: (a) cell viability, (b) cell area, (c) number of neurites per cell, (d) average neurites length. Example of the original images that served for calculation of presented parameters are shown in Fig. S2 in Supporting Information. The error bars represent standard deviation of eight independent data points.

The statistical analysis performed on data on showed no significant difference between samples in all parameters (p value within 0.1 and 0.6 range) except for the parameter number of neurites ($p < 0.001$). However, considering the whole trend during the cell culture, it is clear that all materials support formation of neurites. This part of the study confirmed that all the substrates are suitable for culturing neurons.

3.2 Effect of chemical treatment: PEI, PDL and the role of laminin

Several articles report on successful culturing of neural cells on nanocrystalline diamond^{15, 33, 40}, ultrananocrystalline diamond^{8, 41} or nanodiamond treated substrates⁴² without any form of additional chemical coating. Results of cultivation of uncoated substrates are summarized in⁷.

We did not succeed in culturing primary cortex neurons on materials (glass, gold, NCD2) without a previous polymer treatment. The cell adherence on such materials was extremely low and neurons were not viable (data not shown). It is however possible to successfully enhance cell adherence to the surface and increase attachment of cells with chemical treatment of material before adding the cell suspension. The reason for this behavior was widely discussed and explained in the recent work ²⁶. Chemical treatment can be general to various materials and is usually performed by treating material with selected cationic polymer (most commonly polyethylenimine (PEI) or polylysine (PL)). Additionally to PEI or PL some protocols add laminin to further improve neurite growth and cell adhesion ^{18, 43, 44}.

The goal of this section is to evaluate the impact of the type of the polymer used to promote cell adhesion and development. We compare characteristics of neurons on substrates coated by PEI and by PDL and addition of laminin. As reported by many groups, addition of laminin should improve adhesion of cells to the substrate. The laminin is an important biologically active part of the basal lamina, influencing cell differentiation, migration and adhesion. Laminin has proven to be an influential glycoprotein of the extracellular matrix, which guides and promotes the growth of neurons ⁴⁵. Therefore laminin was added to one series of samples treated by PEI and PDL. The goal was to find out whether laminin is of high importance for the adhesion and development of neurons on diamond thin films.

Results are presented in **Figure 3**. There is not a clear trend in the influence of laminin on the viability. In the case of the PEI and laminin, the viability is lower in comparison to plain PEI. In the case of PDL, the viability is comparable to plain PDL, without any clear trend. Comparing cell area, there is an increase in the cell area for samples treated with laminin and PDL, showing that laminin enhances the cell adhesion and survival in the later days of cultivations, but such trend was not observed for the combination of PEI and laminin. The same trend can be seen also

for the formations of neurites with no clear improvement when laminin was used. The use of laminin does not significantly improves neuron viability and neurite formation when combined with PEI or PDL on diamond thin layers.

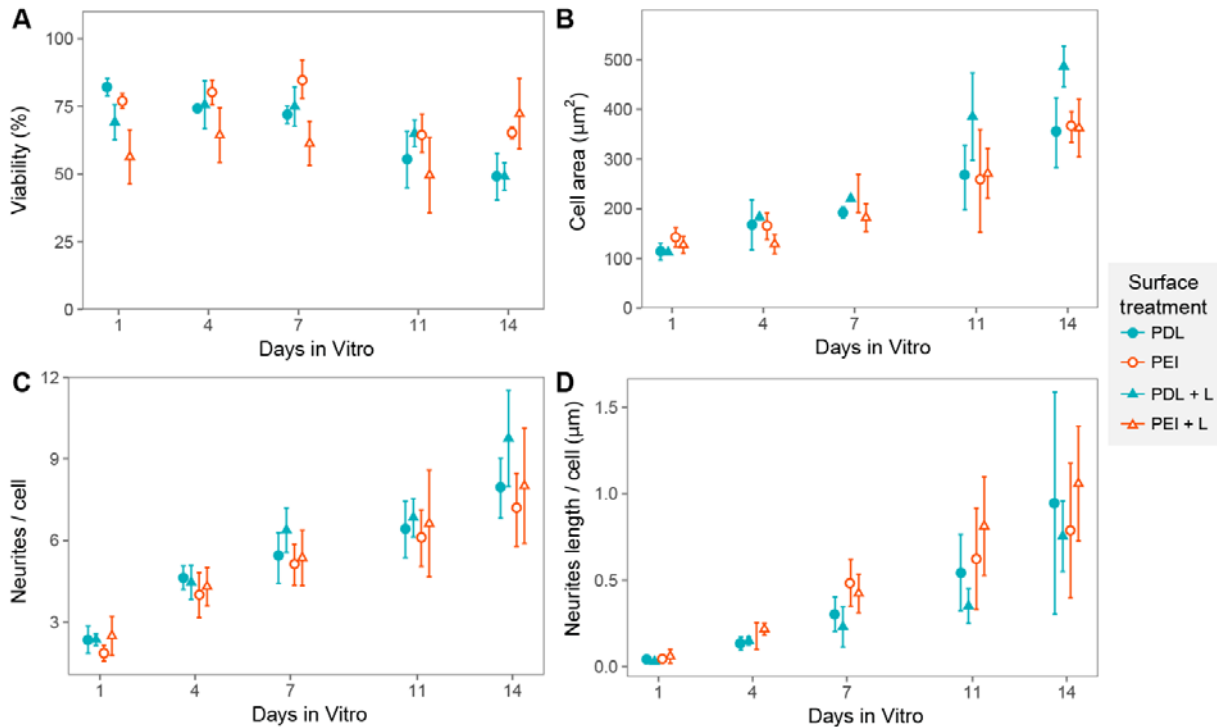


Figure 3. Laminin does not improve significantly the characteristics of neurons and formation of neurites. Graphs show the calculated parameters of neurons cultured on samples coated with poly-D-lysine with laminin (PDL+L), poly-D-lysine without laminin (PDL), polyethylenimine with laminin (PEI+L) and polyethylenimine without laminin (PEI). (a) cell viability, (b) cell area, (c) number of neurites per cell, (d) average neurites length. Example of the original images that served for calculation of presented parameters are shown in Fig. S3 in Supporting information. Glass controls (not included in the graph) showed similar results to the ones on diamond thin films. Cells on controls without coatings showed no live cells after DIV3. Data are not included in the graph for easier visualization. The error bars represent standard deviation of eight independent data points.

Neurons grew successfully on the samples without laminin treatment and therefore laminin does not have to be strictly used for neuron cultivation on NCD films. When comparing PEI and PDL, our results do not show any significant difference in the observed parameters, the results were comparable.

3.3 Effect of chemical treatment: Impact of the molecular weight of polymer

Impact of the molecular weight of PEI was discussed in connection of PEI application as a vector for gene therapy of nervous system, where the toxicity of PEI increases with molecular weight^{46,47}. In this section, we want to examine the impact of a molecular weight of PEI on the adhesion and development of neurons.

We used PEI with three different molecular weights – $M_w = 800 \text{ g mol}^{-1}$ (PEI800), $M_w = 2000 \text{ g mol}^{-1}$ (PEI2000), $M_w = 750000 \text{ g mol}^{-1}$ (PEI750000). The results (Fig. 4) show that the cell characteristics on the PEI800 and PEI2000 treated NCD was comparable for the first 5-7 days of cultivation. After 7 days, samples treated with PEI2000 showed higher viability and better neurite development than samples treated with PEI800 ($p < 0.005$).

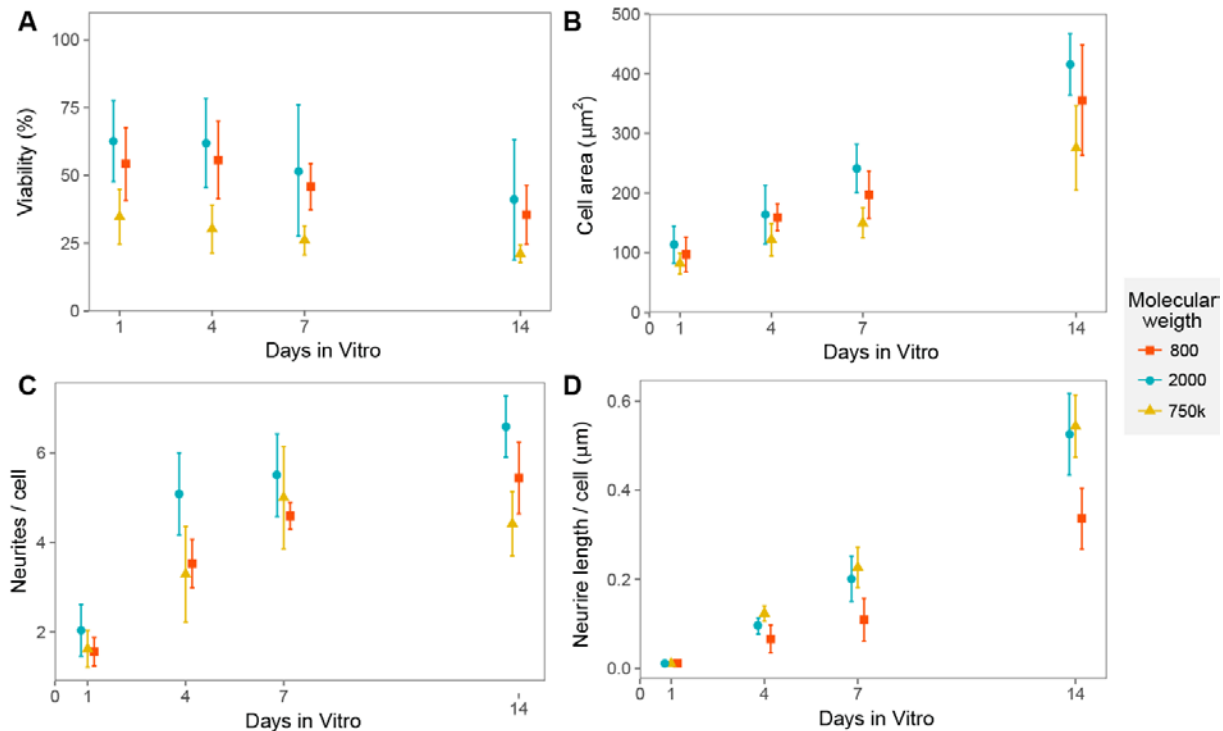


Figure 4. Molecular weight of polyethylenimine affects characteristics of neurons and neurite formation. Graphs show the calculated parameters of neurons cultured on NCD films coated with polyethylenimine of various molecular weight: $M_w = 800 \text{ g mol}^{-1}$ (PEI800), $M_w = 2000 \text{ g mol}^{-1}$ (PEI2000), $M_w = 750000 \text{ g mol}^{-1}$ (PEI750k). (a) cell viability, (b) cell area, (c) number of neurites per cell, (d) average neurites length.

Example of the original images that served for calculation of presented parameters are in Fig. S4 in Supporting information. Glass controls (not included in the figure) showed similar results to the ones on NCD films. Cells on controls without coatings showed no live cells after DIV3. Data are not included in the graph for easier visualization. The error bars represent standard deviation of eight independent data points.

Samples coated with PEI, $M_w = 750\,000\text{ g mol}^{-1}$ (PEI750k) was significantly different from two other sets of samples with lower molecular weight ($p < 0.001$). Cells formed clusters at all samples, also residues of dead cells and tissue were accumulated (Figure S4 in Supporting Information PEI750k). Within a few days and replacement of the culture medium we observed that cell clusters detached and washed off (data not shown).

3.4 Effect of the surface roughness of diamond layers

To understand the impact of morphology on the characteristics of neurons, we compared diamond layers (NCD) of various roughness. We had three sets of samples with different surface RMS roughness from 13 to 32 nm, exact measured values are contained in **Table 3**.

Table 3. Measured RMS values of various nanocrystalline diamond surfaces for neurons culturing. Standard deviance of three independent measurements is given.

Material	RMS (nm)
NCD1	11.6 ± 1.3
NCD2	16.1 ± 1.1
NCD3	31.9 ± 2.6

Besides the difference in the surface roughness (**Figure 5b**), the morphology of the crystalline structure varied. In the case of the NCD1 sample, almost uniform nanocrystal form rod-like grains, while NCD2 and NCD3 samples are polycrystalline layers with various grain sizes and sharp edges (Fig. 5a).

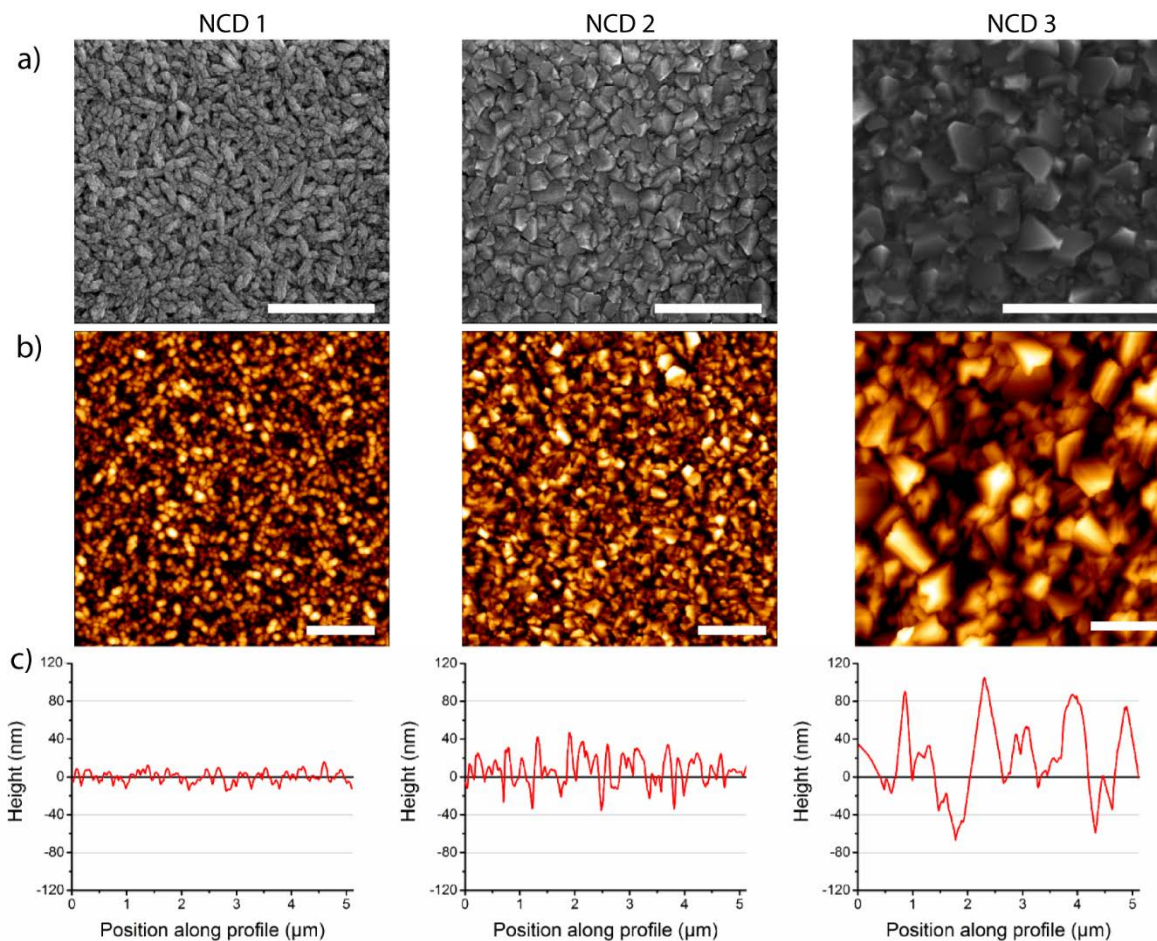


Figure 5. Various surface structure of nanocrystalline diamond layers (NCD) (a) SEM images of NCD samples showing differences in the surface morphology (b) AFM images showing average roughness measured on NCD with $RMS = 13.6$ nm (NCD1), $RMS = 16.1$ nm (NCD2) and $RMS = 31.9$ nm (NCD3). The scale bar is $1 \mu\text{m}$, (b) AFM profiles of the samples ($5 \mu\text{m}$ section taken horizontally across the middle of image).

Prepared diamond layers differ not only in surface morphology, but also in the doping levels of nitrogen and boron (see Table 1 in Materials and Methods for details). Raman spectra (Supplementary materials image S6) show no significant difference in the graphitic content in samples NCD1 and NCD2. Sample NCD3 has significantly lower graphite content, which is typical for layers with larger grain sizes. NCD3 layer has high content of boron and has therefore increased conductivity ($13,7 \Omega\text{m}$). As shown in previous study⁵, the boron content and increased conductivity should have no impact on the neuron development.

Neurons cultivated on NCD samples and the glass control formed neurites from the first day. We observed these phenomena until the end of neuron culturing. Calculated parameters of the viability and neurite growth show a comparable development of neurons cultivated on NCD1 and NCD2 (**Figure 6**). The viability and the cell area was comparable also in the case of NCD3 – the sample with highest surface roughness. However, in this sample, the number and the length of neurites was significantly lower for this sample. The reduced values of neurite development in the samples with highest surface roughness (NCD3) can be caused also by the features in the captured images caused by the lower visibility of the neurites on the samples with high surface roughness (see image S3 in Supporting Information).

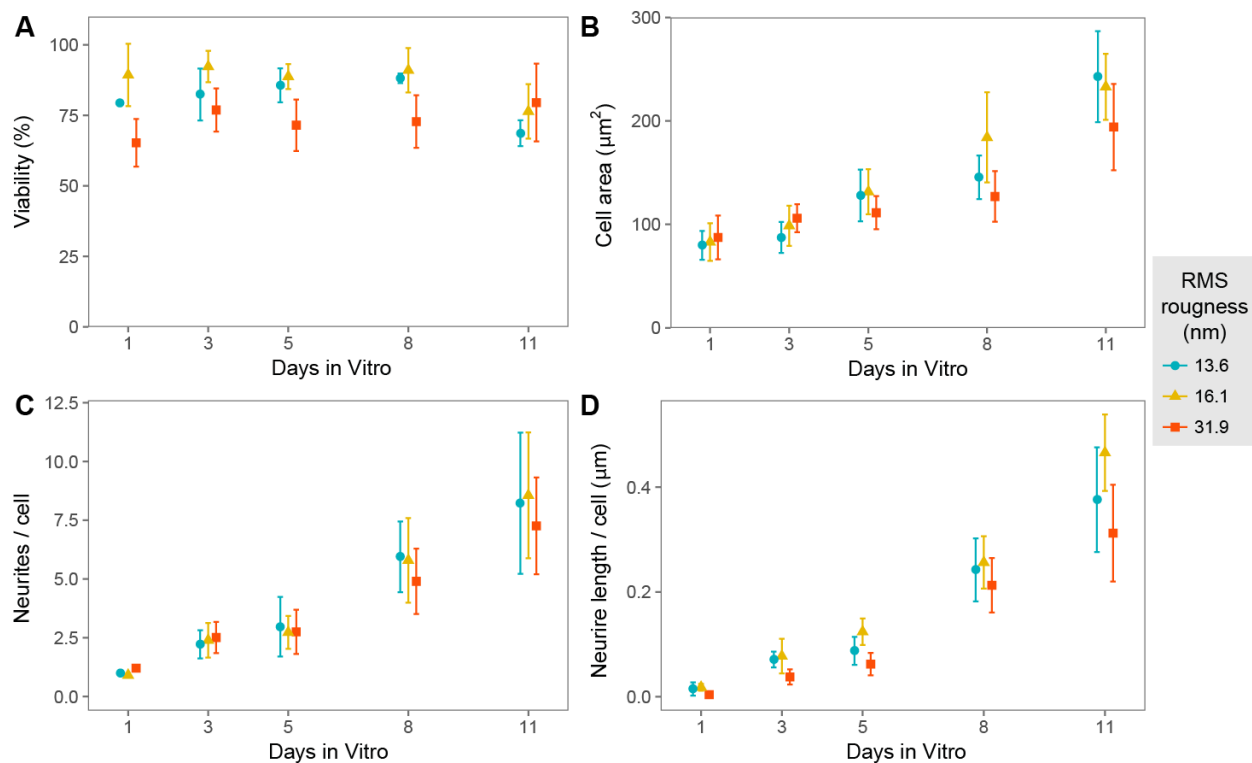


Figure 6. Various surface roughness does not affect significantly the viability and adhesion, and the formation of neurites. Graphs show the resulting parameters from neurons cultured on nanocrystalline diamond layers (NCD) with different surface roughness: RMS = 13.6 nm, (NCD1), RMS = 16.1 nm, (NCD2), RMS = 31.9 nm, (NCD3). Images were obtained at 3, 8, and 11 day “in vitro” (DIV). Scale bar = 50 μm . Graphs

show the results from neuron culturing: (a) cell viability, (b) cell area, (c) number of neurites per cell, (d) average neurites length. Example of the original images that served for calculation of presented parameters are shown in Fig. S5 in Supporting Information. Lower quality of images on NCD3 with highest surface roughness caused lower visibility of neurites and therefore could affect the resulting values of parameters in graph c) and d). The error bars represent standard deviation of eight independent data points.

Based on results reported previously⁴⁰, we expected that a rougher surface will better support the adhesion of neurons. We do not observe such trend and see only minimal variations in the viability and other studied characteristics ($p > 0.05$). It can relate to the difference in the chemical treatment. In the study⁴⁰ no additional coating was performed and different type of cell type (GT1-7) was used. Besides variations in morphology, used diamond films varied in dopants, conductivity, and graphite content (details in Materials and Methods and Supporting information Fig. S6). In the context of previous studies showing no impact of doping and electrical conductivity on the neuron development⁵, our study supports the importance of the chemical treatment on the neuron development over the variations of material properties of diamond thin films such as morphology, doping or electrical conductivity.

4. Conclusions

We have confirmed that nanocrystalline diamond layers are, after the treatment with adhesion-improving polymer, a material that supports adhesion and development of primary neuron cultures with comparable results to gold substrates. All used materials (glass, gold and nanocrystalline diamond) promoted neurons adhesion and formation of neural networks. We have found that variations in surface roughness of nanocrystalline diamond films (within the range of RMS from 11 to 32 nm) does not have a major influence on the neuron viability or adhesion. Surface roughness can affect the formation of neurites. We have further demonstrated that characteristics of neurons can be to some extent be influenced by the type of polymer coating.

Significant impact of the molecular weight of polyethylenimine (PEI) was found. High molecular weight PEI (M_w 750 000) caused cell clumping and neuron characteristics were worse in all studied parameters. Interestingly, in comparison of M_w 800 PEI and M_w 2000 – both very small molecular weights – we have found that in the later days of cultivation neurons developed better on the sample treated with PEI2000. The addition of laminin to films coated with PDL or PEI did not systematically improve neuron adhesion and neurite formation. These findings emphasize the importance of the correct polymer treatment over morphological differences in diamond thin films for the support of neuron adhesion and development.

Supplementary Materials: Supporting material is available

Conflicts of Interest: None

Keywords: diamond thin film, neural interface, surface treatment, surface morphology, biointerfaces

1. G. Piret, C. Hebert, J. P. Mazellier, L. Rousseau, E. Scorsone, M. Cottance, G. Lissorgues, M. O. Heuschkel, S. Picaud, P. Bergonzo, and B. Yvert, *Biomaterials*, 2015, **53**, 173-183.
2. A. C. Taylor, B. Vagaska, R. Edgington, C. Hébert, P. Ferretti, P. Bergonzo, and R. B. Jackman, *Journal of neural engineering*, 2015, **12**(6), 066016.
3. J. M. Halpern, S. T. Xie, G. P. Sutton, B. T. Higashikubo, C. A. Chestek, H. Lu, H. J. Chiel, and H. B. Martin, *Diamond and Related Materials*, 2006, **15**(2-3), 183-187.
4. A. Bendali, L. Rousseau, G. Lissorgues, E. Scorsone, M. Djilas, J. Degardin, E. Dubus, S. Fouquet, R. Benosman, P. Bergonzo, J. A. Sahel, and S. Picaud, *Biomaterials*, 2015, **67**, 73-83.
5. M. Alcaide, A. Taylor, M. Fjorback, V. Zachar, and C. P. Pennisi, *Frontiers in Neuroscience*, 2016, **10**.
6. V. Carabelli, A. Marcantoni, F. Picollo, A. Battiato, E. Bernardi, I. Pasquarelli, P. Olivero, and E. Carbone, *Acs Chemical Neuroscience*, 2017, **8**(2), 252-264.
7. D. J. Garrett, W. Tong, D. A. Simpson, and H. Meffin, *Carbon*, 2016, **102**, 437-454.
8. K. Ganesan, D. J. Garrett, A. Ahnood, M. N. Shivdasani, W. Tong, A. M. Turnley, K. Fox, H. Meffin, and S. Prawer, *Biomaterials*, 2014, **35**(3), 908-915.
9. S. G. Lichter, M. C. Escudie, A. D. Stacey, K. Ganesan, K. Fox, A. Ahnood, N. V. Apollo, D. C. Kua, A. Z. Lee, C. McGowan, A. L. Saunders, O. Burns, D. A. X. Nayagam, R. A. Williams, D. J. Garrett, H. Meffin, and S. Prawer, *Biomaterials*, 2015, **53**, 464-474.
10. T. Lechleitner, F. Klauser, T. Seppi, J. Lechner, P. Jennings, P. Perco, B. Mayer, D. Steinmuller-Nethl, J. Preiner, P. Hinterdorfer, M. Hermann, E. Bertel, K. Pfaller, and W. Pfaller, *Biomaterials*, 2008, **29**(32), 4275-4284.
11. D. J. Garrett, K. Ganesan, A. Stacey, K. Fox, H. Meffin, and S. Prawer, *Journal of Neural Engineering*, 2012, **9**(1).
12. M. Hupert, A. Muck, R. Wang, J. Stotter, Z. Cvackova, S. Haymond, Y. Show, and G. M. Swain, *Diamond and Related Materials*, 2003, **12**(10-11), 1940-1949.
13. L. Kavan, Z. V. Zivcova, V. Petrak, O. Frank, P. Janda, H. Tarabkova, M. Nesladek, and V. Mortet, *Electrochimica Acta*, 2015, **179**, 626-636.
14. Z. V. Zivcova, O. Frank, V. Petrak, H. Tarabkova, J. Vacik, M. Nesladek, and L. Kavan, *Electrochimica Acta*, 2013, **87**, 518-525.
15. A. Bendali, C. Agnes, S. Meffert, V. Forster, A. Bongrain, J. C. Arnault, J. A. Sahel, A. Offenhausser, P. Bergonzo, and S. Picaud, *Plos One*, 2014, **9**(3).
16. P. W. May, E. M. Regan, A. Taylor, J. Uney, A. D. Dick, and J. McGeehan, *Diamond and Related Materials*, 2012, **23**, 100-104.
17. E. M. Regan, A. Taylor, J. B. Uney, A. D. Dick, P. W. May, and J. McGeehan, *Ieee Journal on Emerging and Selected Topics in Circuits and Systems*, 2011, **1**(4), 557-565.
18. C. G. Specht, O. A. Williams, R. B. Jackman, and R. Schoepfer, *Biomaterials*, 2004, **25**(18), 4073-4078.
19. F. G. Celii and J. E. Butler, *Annual Review of Physical Chemistry*, 1991, **42**, 643-684.
20. J. E. Butler, Y. A. Mankelevich, A. Cheesman, J. Ma, and M. N. R. Ashfold, *Journal of Physics-Condensed Matter*, 2009, **21**(36).
21. O. A. Williams, M. Nesladek, M. Daenen, S. Michaelson, A. Hoffman, E. Osawa, K. Haenen, and R. B. Jackman, *Diamond and Related Materials*, 2008, **17**(7-10), 1080-1088.
22. R. K. Roy and K. R. Lee, *Journal of Biomedical Materials Research Part B-Applied Biomaterials*, 2007, **83B**(1), 72-84.
23. M. Amaral, P. S. Gomes, M. A. Lopes, J. D. Santos, R. F. Silva, and M. H. Fernandes, *Journal of Nanomaterials*, 2008.
24. M. Amaral, A. G. Dias, P. S. Gomes, M. A. Lopes, R. F. Silva, J. D. Santos, and M. H. Fernandes, *Journal of Biomedical Materials Research Part A*, 2008, **87A**(1), 91-99.

25. V. Kočka, T. Jirásek, A. Taylor, F. Fendrych, B. Rezek, Z. Šimůnková, I. Mrázová, P. Toušek, J. Mistrík, V. Mandys, and M. Nesládek, *Novel nanocrystalline diamond coating of coronary stents reduces neointimal hyperplasia in pig model*. 2014: Experimental and Clinical Cardiology. p. 65-76.
26. S. M. Ojovan, M. McDonald, M. McDonald, N. Rabieh, N. Shmuel, H. Erez, M. Nesladek, and M. E. Spira, *Frontiers in neuroengineering*, 2014, **7**, 17-17.
27. F. Vahidpour, L. Curley, I. Biró, M. McDonald, D. Croux, P. Pobedinskas, K. Haenen, M. Giugliano, Z. V. Živcová, and L. Kavan, *physica status solidi (a)*, 2017, **214**(2).
28. M. McDonald, A. Monaco, F. Vahidpour, K. Haenen, M. Giugliano, and M. Nesladek, *Mrs Communications*, 2017, **7**(3), 683-690.
29. C. Hébert, J. P. Mazellier, E. Scorsoni, M. Mermoux, and P. Bergonzo, *Carbon*, 2014, **71**, 27-33.
30. V. Petrák, Z. V. Živcová, H. Krýsová, O. Frank, A. Zupal, L. Klimša, J. Kopeček, A. Taylor, L. Kavan, and V. Mortet, *Carbon*, 2017, **114**, 457-464.
31. A. C. Taylor, C. H. González, B. S. Miller, R. J. Edgington, P. Ferretti, and R. B. Jackman, *Scientific Reports*, 2017, **7**(1), 7307.
32. M. Alcaide, S. Papaioannou, A. Taylor, L. Fekete, L. Gurevich, V. Zachar, and C. P. Pennisi, *Journal of Materials Science-Materials in Medicine*, 2016, **27**(5).
33. O. Babchenko, N. Romanyuk, P. Jendelova, and A. Kromka, *Physica Status Solidi B-Basic Solid State Physics*, 2013, **250**(12), 2717-2722.
34. A. Taylor, F. Fendrych, L. Fekete, J. Vlcek, V. Rezacova, V. Petrak, J. Krucky, M. Nesladek, and M. Liehr, *Diamond and Related Materials*, 2011, **20**(4), 613-615.
35. M. J. Krecmarova, V. Petrak, A. Taylor, K. J. Sankaran, I. N. Lin, A. Jager, V. Gartnerova, L. Fekete, J. Drahokoupil, F. Laufek, J. Vacik, P. Hubik, V. Mortet, and M. Nesladek, *Physica Status Solidi a-Applications and Materials Science*, 2014, **211**(10), 2296-2301.
36. M. Pacifici and F. Peruzzi, *Jove-Journal of Visualized Experiments*, 2012(63).
37. G. J. Brewer, J. Torricelli, E. Evege, and P. Price, *Journal of neuroscience research*, 1993, **35**(5), 567-576.
38. A. Hai, J. Shappir, and M. E. Spira, *Nature Methods*, 2010, **7**(3), 200-U250.
39. G. Panaitov, S. Thiery, B. Hofmann, and A. Offenhausser, *Microelectronic Engineering*, 2011, **88**(8), 1840-1844.
40. P. Ariano, O. Budnyk, S. Dalmazzo, D. Lovisolo, C. Manfredotti, P. Rivolo, and E. Vittone, *European Physical Journal E*, 2009, **30**(2), 149-156.
41. A. Voss, H. Wei, C. Mueller, C. Popov, W. Kulisch, G. Ceccone, C. Ziegler, M. Stengl, and J. P. Reithmaier, *Diamond and Related Materials*, 2012, **26**, 60-65.
42. A. Thalhammer, R. J. Edgington, L. A. Cingolani, R. Schoepfer, and R. B. Jackman, *Biomaterials*, 2010, **31**(8), 2097-2104.
43. P. A. Nistor, P. W. May, F. Tamagnini, A. D. Randall, and M. A. Caldwell, *Biomaterials*, 2015, **61**, 139-149.
44. E. Fusaoka-Nishioka, C. Shimono, Y. Taniguchi, A. Togawa, A. Yamada, E. Inoue, H. Onodera, K. Sekiguchi, and T. Imai, *Neuroscience Research*, 2011, **71**(4), 421-426.
45. H. K. Kleinman, L. Luckenbilledds, F. W. Cannon, and G. C. Sephel, *Analytical Biochemistry*, 1987, **166**(1), 1-13.
46. G. P. Tang, H. Y. Guo, F. Alexis, X. Wang, S. Zeng, T. M. Lim, J. Ding, Y. Y. Yang, and S. Wang, *Journal of Gene Medicine*, 2006, **8**(6), 736-744.
47. F. C. Perez-Martinez, B. Carrion, and V. Cena, *Journal of Alzheimers Disease*, 2012, **31**(4), 697-710.